How effective are reducing plasma afterglows at atmospheric pressure in removing sulphide layers : application on tarnished silver, sterling silver, and copper

How effective are reducing plasma afterglows at atmospheric pressure in removing sulphide layers: application on tarnished silver, sterling silver and copper

Olivier Schalm[1], Patrick Storme[1], Arianna Gambirasi[2], Monica Favaro[2], Alessandro Patelli[3]

1: University of Antwerp, Conservation Studies, Blindestraat 9, B-2000 Antwerp, Belgium
2: Consiglio Nazionale delle Ricerche, Istituto di Chimica Inorganica e delle Superfici, Corso Stati Uniti 4, 35127 Padova, Italy
3: Padova University, Department of Physics and Astronomy, via Marzolo 8, 35122 Padova, Italy

Corresponding author:
University of Antwerp
Conservation Studies
Blindestraat 9
B-2000, Antwerp, Belgium
Phone: +32 (0)3 213 71 34
olivier.schalm@uantwerpen.be

Abstract

A plasma afterglow from a gas mixture of 5 vol% H_2 in He is able to remove tarnish layers on pure silver in a matter of seconds. This dry, localised and non-contact cleaning technique is a promising method to clean historical objects where silver is combined with organic materials and where traditional cleaning techniques are not recommended. However, historical objects are often manufactured with silver alloys but somehow their tarnish layers are removed less effectively with plasma treatments. In order to understand the different impact of the afterglow, the surfaces of corroded silver, sterling silver and copper coupons are characterized before and after plasma treatment by a multi-analytical approach combing optical and confocal microscopy, scanning electron microscopy coupled to energy dispersive X-ray analysis and chronopotentiometry. The analyses demonstrate that the few hundred nanometres thick tarnish layer on pure silver is transformed through the whole thickness resulting in a porous metallic film. On top of that metallic film, some isolated remnant Ag_2S particles are found. For sterling silver, a yellowing of the surface occurs. The Ag-rich corrosion products are reduced to a large extent, while the Cu-rich corrosion products are only partially reduced. For corroded copper, no apparent visual change is observed at a macroscopic scale, although the morphology of the surface changed. The results allow an evaluation of the cleaning efficiency and provide a deeper understanding of hydrogen plasma effects on the transformation of sulphide tarnish layers at atmospheric pressure.

Keywords

cleaning efficiency, corrosion, cultural heritage, plasma afterglow, sterling silver, sulphide

1. Introduction

In the conservation-restoration of objects of art, undesired layers (e.g., soot, discoloration of silver due to the formation of a tarnish layer, yellowed varnishes) often have to be removed from surfaces. In the case of genuine silver alloy objects, several well-established cleaning techniques exist to remove tarnish layers and to regain the original lustre [1]. Examples of such techniques are silver dip (i.e., a solution containing thiourea as complexing agent) [2], reductive agents [3], electrochemical reduction [4,5] or polishing techniques. Unfortunately, these well-established cleaning techniques are not recommended when organic materials are in close contact with tarnished silver (e.g., silver threads in textile, silver foils on wooden statues, or photographic glass negatives) because they result in the unavoidable chemical attack or mechanical abrasion of the very sensitive organic materials. Another example where well-established cleaning techniques resulted in permanent damage is the treatment of daguerreotypes (i.e., the first photographic plates introduced by Louis Jacques Mandé Daguerre in 1839) with cyanide or thiourea solutions. These treatments were once popular but several years later, it became clear that in some cases the cleaning caused accelerated fading. It brought traditional methods into disrepute so that in the 1970's a general recommendation was made that daguerreotypes should not be cleaned at all [6,7].

Plasma treatments have been proposed as an alternative dry and non-contact cleaning technique for quite some time. Both plasma treatments at low pressure [8] and afterglows containing hydrogen radicals and/or ro-vibrationally excited hydrogen molecules are able to reduce Ag_2S-layers [9]. Also tarnish layers of silver alloys can be reduced with low pressure plasmas [10-14]. These experiments suggest that this method might be used for the cleaning of mixed media objects containing pure silver, as is the case of daguerreotypes [15] or paper-based photographs [16]. Despite the large experience with low pressure plasmas, this technique is often not suited for heritage applications. Usually the objects are too large for a closed chamber. In addition, low pressure conditions can damage fragile objects. Therefore, an atmospheric pressure plasma torch would be more advantageous. Such torches are very efficient for tarnish layers on top of pure silver [17-18] but tarnish layers on silver alloys that are visually very similar to the ones on pure silver are much harder to remove. This reduced cleaning efficiency might be the result of the preferential oxidation of the small amounts of copper in silver alloys, resulting in Cu-rich tarnish layers [19]. It is possible that the compounds present in the tarnish layer are not affected in the same way when exposed to an atmospheric pressure plasma.

In order to understand these variations in cleaning efficiency an atmospheric pressure plasma is tested on artificially corroded silver (Ag999 contains at least 99.9 w% Ag), sterling silver (Ag925 consists of 92.5 w% Ag and Cu 7.5 w% Cu) and copper (Cu999 contains at least 99.9 w% Cu). The plasma torch is used with a reducing feeding gas of 5 vol% H_2 in He and samples are treated in the plasma afterglow to avoid streamers effects. The surfaces of the corroded metal coupons are characterized before and after the plasma treatment by means of a multi-analytical approach combining optical and confocal microscopy, scanning electron microscopy coupled to an energy dispersive X-ray spectrometer and chronopotentiometry. From these analyses, the cleaning efficiency for individual compounds in the tarnish layer can be evaluated and the reduction processes can be drawn.

2. Background

It is a common practice to select the most appropriate cleaning method by performing a comparative evaluation of several well-established cleaning methods. Such an evaluation is often based on small cleaning tests performed at an inconspicuous location on the artwork. The assessment of treated zones is usually an appreciation of the visual appearance of the surface. However, this method is not a scientific basis for the exploration of experimental cleaning methods. Moreover, the heritage community does not allow the application of experimental cleaning techniques on genuine historical objects [20]. For that reason, the exploration of experimental cleaning methods has to be performed on artificial corroded coupons. Two different approaches exist to define cleaning efficiency: (1) the cleaned surface is compared with the surface before cleaning in the corroded state and the unwanted layer should be removed as much as possible, and (2) the cleaned surface is compared to its original state and should approach that state as close as possible [21,22].

- **Approach 1:** An excellent cleaning efficiency means that the difference between the corroded surface and the cleaned surface is as large as possible. In this approach, a surface property q must be selected that is proportional with the extent of corrosion. The quantity q corresponding to corrosion state is set to 100% and must be lowered as much as possible. The cleaning efficiency can be calculated by the formula given below.

$$\text{Efficiency} = \frac{|q_{corroded} - q_{cleaned}|}{q_{corroded}} \times 100\%$$

- **Approach 2:** Good cleaning efficiency means that the difference between the original polished coupon and the cleaned surface is as small as possible. In this approach, the original state 1 corresponds to 100%.

$$\text{Efficiency} = 100\% - \frac{|q_{cleaned} - q_{original}|}{q_{original}}$$

Since visual appreciation plays an important role in cleaning evaluations, it seems logic to use surface colour (i.e., discoloration is related to the extent of corrosion) or gloss (i.e., this is related to the surface roughness of the surface) as a surface property q_i. However, it is also possible to use other criteria based on in depth assessments of chemical composition, microstructure and topography [23,24]. For example, the surface concentration of sulphur can be used to determine the cleaning efficiency. It should be highlighted that the cleaning efficiency is highly affected by the choice of the parameter. For example during cleaning, the sulphide concentration should be lowered while the gloss should be enhanced. However, the corrosion process affects the surface morphology so that even when all sulphides are removed gloss cannot be completely regained. In the following, approach 1 will be used for the cleaning evaluation because for historical objects the original state is often unknown. In addition, as surface property q_i have been chosen the transition times of the chronopotentiometry.

3. Material and methods

3.1. Materials

Coupons (20 mm x 50 mm) are cut from larger sheets of Ag999, Ag925 and Cu999 using a parallel metal cutting guillotine. The silver sheets Ag925 and Ag999 are purchased at Schöne Edelmetaal B.V. (Netherlands), which retrieves its metal from Degussa, Germany. The sheets of Cu999 are obtained from Dejond Metals nv, Antwerp (Belgium). An inventory number is engraved at the backside of the coupons. The front side is grinded and polished with a fixed procedure to obtain as close as possible identical surface states. On the surface of the coupon, a small amount of water soluble polishing pastes (3M™ Finesse-it™ Finishing Material, followed by 3M™ Imperial™ Machine Glaze) is applied and the surface is brought into contact with a soft cotton rotating wheel for approximately 1 minute. Cleaning of the polished surface is performed by immersing the coupon in an ultrasonic bath with ethanol for 2 minutes. Afterwards, the coupons are rinsed with deionised water and dried with oil- and water-free compressed air [25]. The mirror-like appearance of the surface is very similar to that of historical 'silver' objects finished with a traditional mechanical and abrasive polishing technique [1,26,27].

For the artificial corrosion, the coupons are exposed to subsequent cycles consisting of a short immersion (12 s for every cycle of 60 s) in a Na_2S solution (0.1 mol/L $Na_2S.9H_2O$, pH = 14) followed by a longer exposure to air (48 s/60 s cycle) [25]. Dissolved sulphides are known to make the solutions alkaline. For Ag999, Ag925 and Cu999 the exposure time is respectively 300 minutes, 60 minutes and 30 minutes. The exposure time must be diminished for the metals with higher copper amounts in order to compensate for the higher corrosion rates. All tarnish layers have a black and dull appearance and are well attached to the surface.

A dielectric barrier discharge commercial plasma-jet, type Plasma Spot®, is used for the experiments. The power is set to 120 W with a gas flow of 70 slm (standard liter per minute). The nozzle of the torch has a circular opening with a diameter of 10 mm. Inside that opening, a central anode of 6 mm diameter is located. For the removal of the tarnish layer, a reducing gas mixture of 5 vol% H_2 in He is used. The plasma-jet is mounted perpendicular to the coupons with a working distance of 5 mm. The treated area is approximately 15 mm in diameter. The cleaning time varies between 15 s and 120 s. During the treatment, the samples reached a maximum temperature of 50-70°C. In the remote configuration used in the present plasma setup the sample is not seen as an electrode. The setup has been chosen in order to avoid the potential reducing effect of the current coming from the plasma and passing through the sample surface.

Some comparative cleaning tests are performed with silver D.7 solution. This type of silver dip is made by mixing 8 g thioureum with 1.1 ml HCl solution of 37 vol%, 0.5 ml non-ionic surfactant Triton X-100 and 86.4 ml distilled water [28].

3.2. Microscopic and chemical characterization of the surfaces

The corroded coupons are analysed before and after the plasma treatments using a multi-analytical approach. The evaluation consists of a visual, microscopic and chemical inspection of the surfaces. From these analyses, surface properties are determined that allowed the evaluation of the cleaning efficiency.

- **Visual appearance:** The visual appearance is evaluated by collecting photos from the coupons. Surface topography and roughness is analyzed with a confocal laser scanning microscope LEXT OLS4100 of Olympus, images are collected in bright field and in intensity mode. This technique allows the creation of a three-dimensional representation of the surface and height profiles are extracted.
- **Surface roughness:** The surface roughness is calculated using the arithmetic deviation from the mean line (Ra) after removing the contribution of longer wavelengths (> 8 µm). Except for the tarnish layer of Ag999, none of the surfaces endured irradiation damage by the 405 nm laser. This damage can be seen as a rectangular discoloration of the area analysed. The Mitutoyo surface micro-roughness tester SJ-201 has been used as a supplementary method to measure surface roughness.
- **Microstructure:** The surfaces microstructure are visualized with an Olympus DSX510 optical microscope by bright field. By creating a z-stack with the Extended Focal Image (EFI) function, high resolution colour images are acquired at elevated magnification. The surfaces are also examined with a Quanta 200 F field emission - Scanning Electron Microscope equipped with an EDAX energy dispersive X-ray spectrometer (FE-SEM-EDS). Quantitative analysis of the tarnish layers is not reliable because photons are also generated from the bulk metal below. A three-dimensional view of the surface is obtained by tilting the sample at 75°. Chemical analyses are performed by EDS at an electron accelerating voltage of 20kV.
- **Chemical speciation:** The surface concentration of the compounds in a tarnish layer can be determined by chronopotentiometry [29]. The complete reduction of the tarnish layer is performed in a three-electrode cell in which the coupon is the working electrode and a platinum grid the counter electrode. A Saturated Mercurous Sulphate Electrode (MSE; Hg/Hg_2SO_4/saturated K_2SO_4; 0.615 V versus standard hydrogen electrode) is used as reference electrode. The three-electrode cell contains a small aperture of 5 mm diameter (i.e., 0.2 cm^2) which gives access to the coupon surface. The cell is filled with a 0.1 mol/L $NaNO_3$ solution. This electrolyte is a good conductor and does not chemically attack the metals. It has been used for electrochemical cleaning of tarnished silver objects [30,31]. The measurements are performed with a Palmsens potentiostat/galvanostat. The chronopotentiometric analyses of the tarnish layers are performed by applying a constant current of -100 µA while the voltage needed to provide that current is measured over time with a step size of 0.1 s. The height of the distinctive plateaus in the potentiograms are used to identify the corrosion products. The length of time over every plateau is proportional to the surface concentration of the corresponding corrosion product. These lengths are determined from the first derivative of the chronopotentiograms obtained with a 25-point Golay-Savitzky filter after curve smoothing.

4. Results

4.1. Interaction between the plasma afterglow and Ag999

The photo in Fig. 1a shows a corroded coupon. In the centre of that coupon a circular zone can be seen that is treated with a reducing plasma for 15 s. A clear difference between the two zones can be seen. Visually, the treated surface is brighter and glossier, although the original gloss of polished silver is not achieved.

The surface of the sample before the plasma treatment shows the presence of grains of about 2.5 µm on top of an apparently granular and rough film (fig. 1b and 1d). The crystal grains over the corroded surface appear black in the bright field optical microscope image, while in the SEM crystal facets are clearly observed. After the plasma treatment, the images in Fig. 1c suggest that the grains are still present on top of the surface as dark spots, but the background colour disappeared. The effect of the treatment on surface is clearer in SEM image (fig. 1e) where both surface and top grains endured a morphological change. The images collected at higher magnification and shown in Fig. 1f and 1g give a better insight in the morphology of the surface. Before the plasma treatment the tarnish layer consists of a random packing of grains with a diameter of about 0.2 µm with some larger grains of about 1 µm (Fig. 1f), while after the plasma process the surface is transformed into a porous film (Fig. 1g). Also the grains on the top of the surface are affected by the plasma treatment, crystal facets are less visible and seem to be covered by the same porous coating as the surface below.

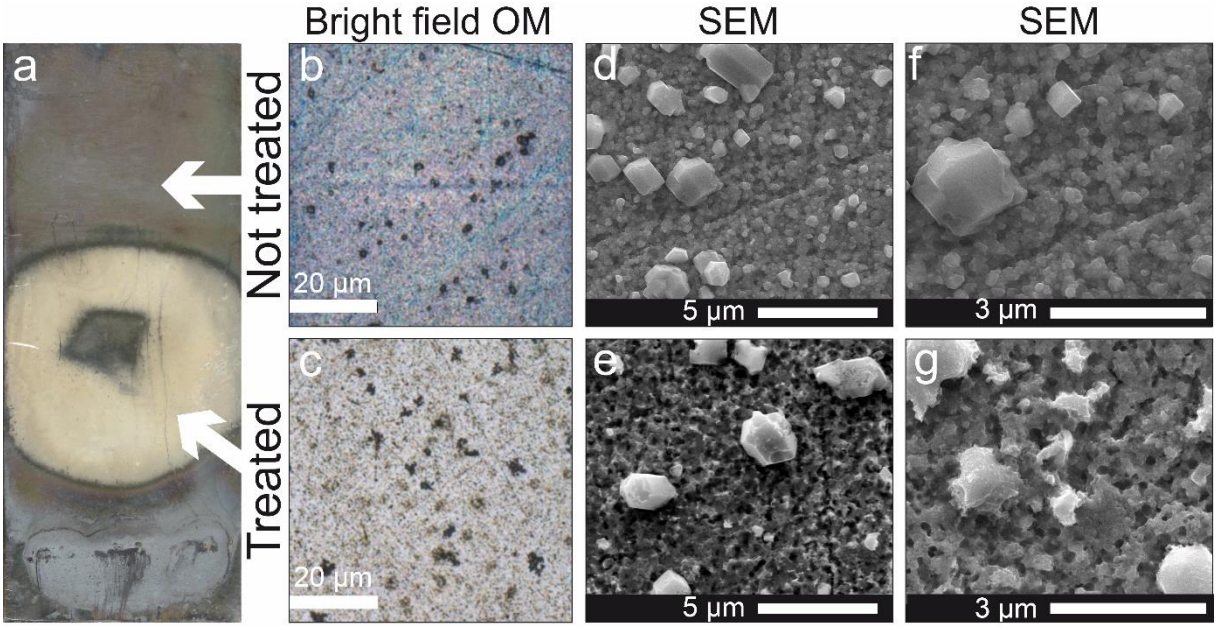

Fig. 1: Inspection of the corroded surface before and after plasma treatment. a) Photo of the corroded coupon. White arrows indicate the not treated and treated areas analysed; b) Bright field image collected with the optical microscope of the corroded surface and c) of the cleaned area; d) Secondary electron image of the corroded surface and e) of the plasma treated area; f) Secondary electron of a larger grain on top of the tarnish layer and g) remnant of such a grain after plasma treatment.

The height maps (Fig. 2) show that the surface roughness of corroded Ag999 before and after the plasma treatment remains in the same order of magnitude even if the morphology has changed. The average surface roughness Ra before and after the treatment is about 12 nm. The grains on top of the surface are always in the micrometre size range. Therefore, the chemical reduction process it is not smoothing the surface. Moreover, in the treated area some holes appear in the nanometre range (i.e., the sudden drops in the profile), which perhaps correlate with the increase of the reduced surface porosity..

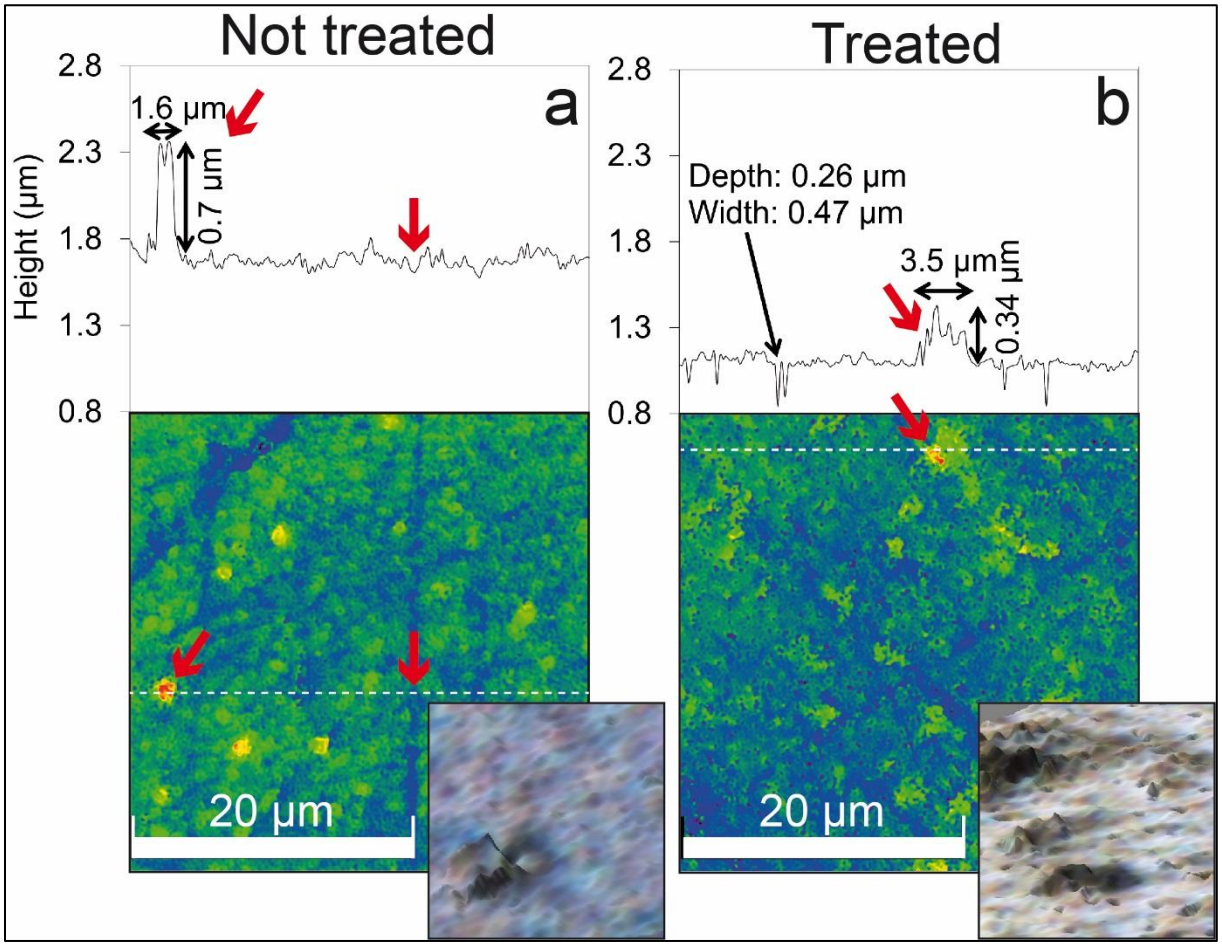

Fig. 2: Topography of corroded Ag999 before and after plasma treatment as obtained by confocal microscopy. a) Height map of the tarnish layer, height profile along the dotted line and 3D visualization of the surface; b) Height map of a plasma treated area, height profile along the line showing bumps and pores and 3D visualization of the surface showing the presence of pores.

The EDS spectra in Fig. 3a from the tarnish layer shows that the sulphide signal disappeared after cleaning while a higher oxygen content is observed. This means that the Ag_2S is reduced into metallic Ag. The corresponding oxidation reaction must be the transformation of excited H_2 molecules into H^+ ions. These ions explain the formation of H_2S in the exhaust of the reactor [9]. Therefore, the porous morphology that is characteristic after the plasma treatment and that can easily be observed in the SEM images must be formed during the conversion to the metallic state. Since at low temperature and in dry environment there is no possibility for silver atom to

rearrange on a macroscale in a matter of seconds, the sudden drop in molar volume must lead into a porous metallic film. However not all the silver sulphide is fully reduced. The larger grains on top of the surface seems to be chemically unaffected by the afterglow during the short treatment time (see Fig. 3b), although the morphology of the grains has changed (see Fig. 1g). Therefore, the reduction seems to involve only the surface in the hundred nanometer range. The presence of oxygen can either be due to the formation of reactive oxygen species when the afterglow is mixed with air or it may be due to air exposure after the plasma treatment where the surface of the highly porous metal is covered by oxides.

The chronopotentiometry analyses and the first derivative of the chronopotentiograms in Fig. 3c show the presence of a single compound. There is only one plateau at -1.3 V vs. MSE and this corresponded with Ag_2S. The transition times are cleared seen and are used as a physical property to estimate the cleaning efficiency using approach 1. The efficiency is about 87 %, which is coherent with the presence of remnants of silver sulphide grains on the top of the surface after cleaning.

The cross section of the corroded Ag999 layer before the plasma treatment shown in Fig. 3d is the result of the sulphidation process with an exposure time of 300 minutes. It can be seen how the corrosion leads to a roughening of the surface and to a creation of a silver sulphide layer of about 220 nm. Therefore the size of the pores observed in Fig. 2b is of the order of magnitude of the thickness of the tarnish layer. When Ag999 is corroded at different exposure times, the surface roughness as determined by the surface roughness tester increases with the exposure time. For exposure times below 300 minutes, the surface roughness remains small and plasma treatments appear to work well; for longer exposure times the surface roughness increases strongly and the efficiency of the plasma treatments drops. Moreover the dark grey colour of the tarnish layer is only partially changed. The plasma treated tarnish layers are later submitted to a silver dip treatment, a widely used product in the heritage community, to remove the remaining corrosion products. As a consequence of that, the surface roughness dropped substantially. However, even when the tarnish layer has completely been removed by the silver dip the original gloss of the metal could not be regained. This means that the corrosion process has an etching effect and that without polishing the surface, it is impossible to regain the original gloss.

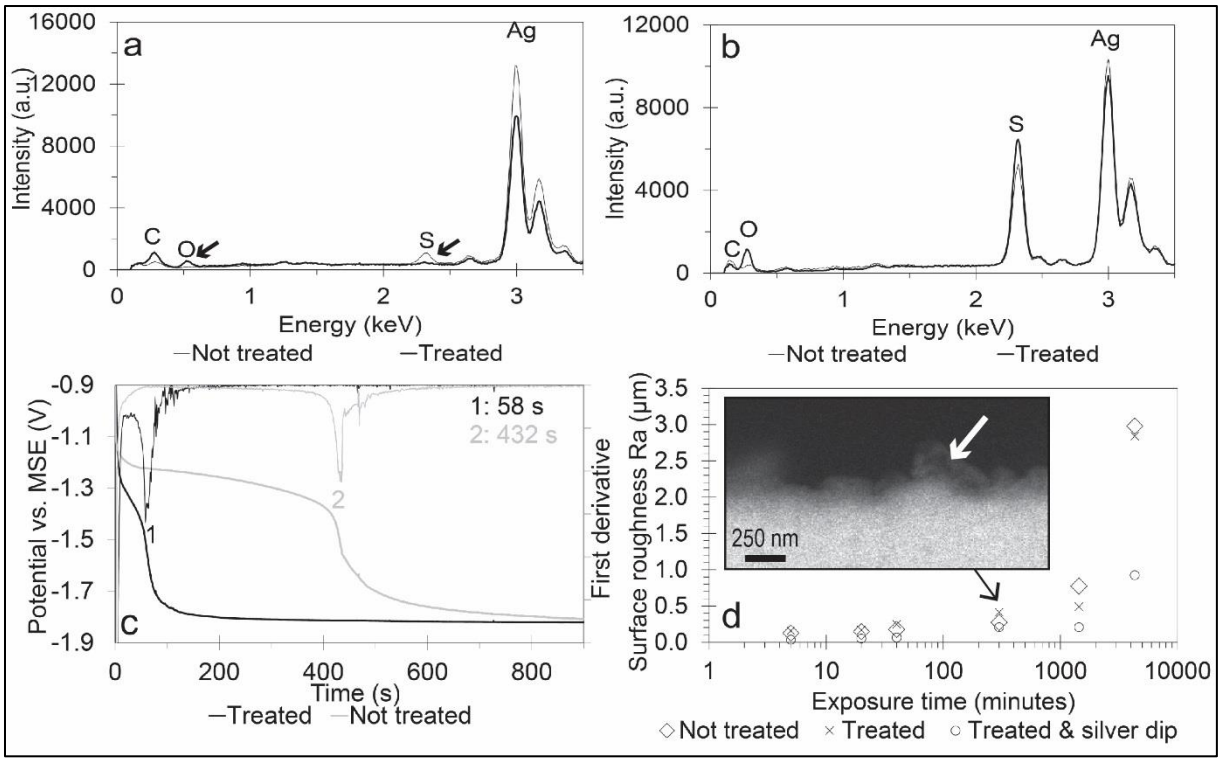

Fig. 3: Surface analyses of Ag999: a) EDS spectra from the tarnish layer before and after plasma treatment; b) EDS spectra of the larger grains on top of the surface before and after plasma treatment; c) Chronopotentiometry of corroded Ag999 before and after plasma treatment and the corresponding first derivative used to calculate the transition times; d) Average surface roughness of the corroded surface as a function of exposure time to the Na_2S solution, roughness after cleaning with plasma, and roughness of the plasma treated area after treatment with silver dip. On the inset, cross-section of Ag999 after an exposure time of 300 minutes. The tarnish layer is the irregular darker layer at the white arrow.

4.2. Interaction between the plasma afterglow and Ag925

The photo of the corroded Ag925 coupon in Fig. 8a shows that the plasma afterglow transforms the corroded layer to a yellowish, pinkish or brownish surface. Despite the fact that the surface changes drastically during plasma treatment, the final colour is unsatisfactory in regard to polished Ag925, that is supposed to be a near-colourless mirror.

In order to understand the discoloration and to improve the plasma cleaning technology, it is necessary to characterize this transformation in depth. The bright field image (Fig. 4b), the secondary electron image (in Fig. 4d and 4f), the confocal image (Fig. 5a) and the EDS spectra of Fig. 6 show that the tarnish layer consists of 3 phases: (1) The Cu-rich platelets correspond to the black zones in Fig. 4b because in Fig. 5a the elevated zones are black, (2) The grey zones around the platelets correspond with the Cu-rich bumps, and (3) the coloured zones (see Fig 4b) correspond with the valleys as suggested in Fig. 5a. After plasma treatment, the coloured valleys disappear and are replaced by a brighter yellowish phase, while the grey phase becomes darker. The coloured phase in the lower areas becomes clearly brighter but the darker zones that protruded above the surface are unaffected by the plasma treatment. A three-dimensional view is also obtained with SEM-EDX by tilting the sample. In Fig. 4f, the platelets protruding

the surface appears to be almost perpendicular to the surface. Besides these crystals, also bumps can be seen. After plasma treatment, the number of platelets are strongly reduced but the small bumps remain (Fig. 4g).

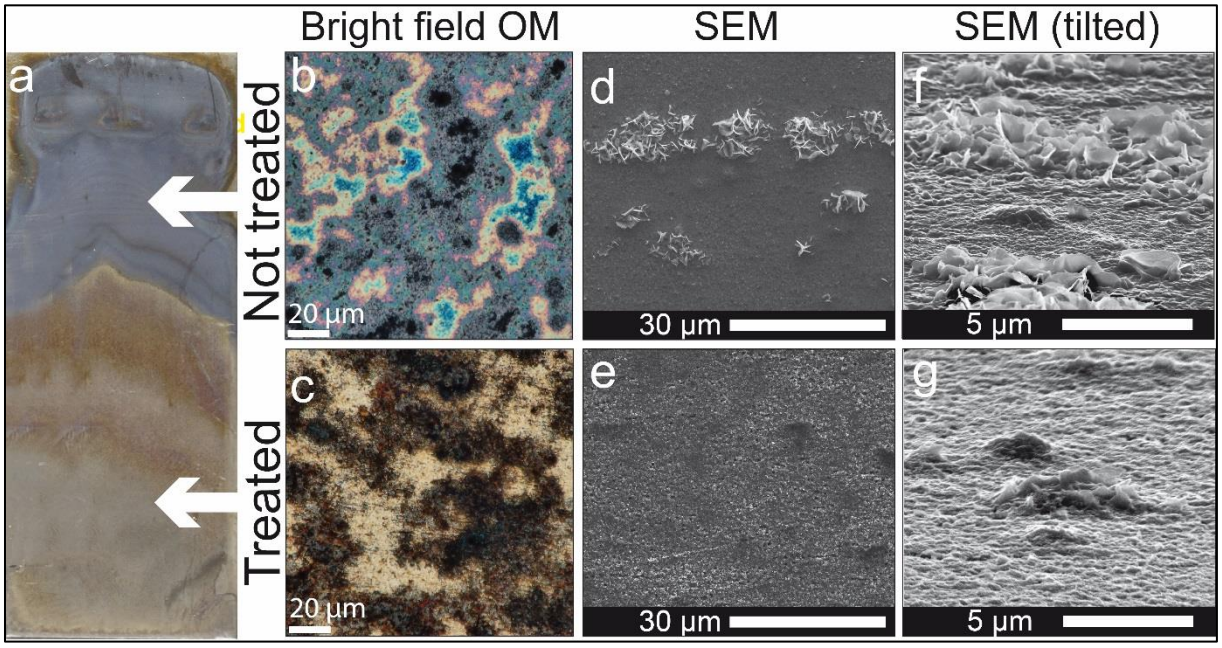

Fig. 4: Inspection of the corroded and plasma treated Ag925 surface. a) Corroded coupon locally treated by plasma resulting in a visually poor cleaning (see white arrow); b) Bright field image collected by optical microscopy of the tarnish layer and where 3 phases can be recognized; c) Bright field image of the plasma treated tarnish layer and where only 2 phases can be recognized; d) Secondary electron image of the tarnish layer visualizing the granular morphology of that layer with on top platelets; e) Secondary electron image of the surface of the plasma treated tarnish layer also showing a granular surface; f) Secondary electron image of the tilted sample showing Cu-rich flat platelets and bumps; d) Secondary electron image of the tilted sample after plasma treatment where Cu-rich bumps are still present but where the platelets have mostly disappeared.

The height maps in Fig. 5 clearly show that the crystals rise well above the surface while the coloured areas are located in the valleys. This analysis demonstrates that the corrosion process turns the polished mirror-like surface in a surface with variating topography. There is a clear correlation between height and colour. During plasma treatment, the coloured valleys become smoother and yellow. The dark zones remain dark and have a higher roughness than the valleys.

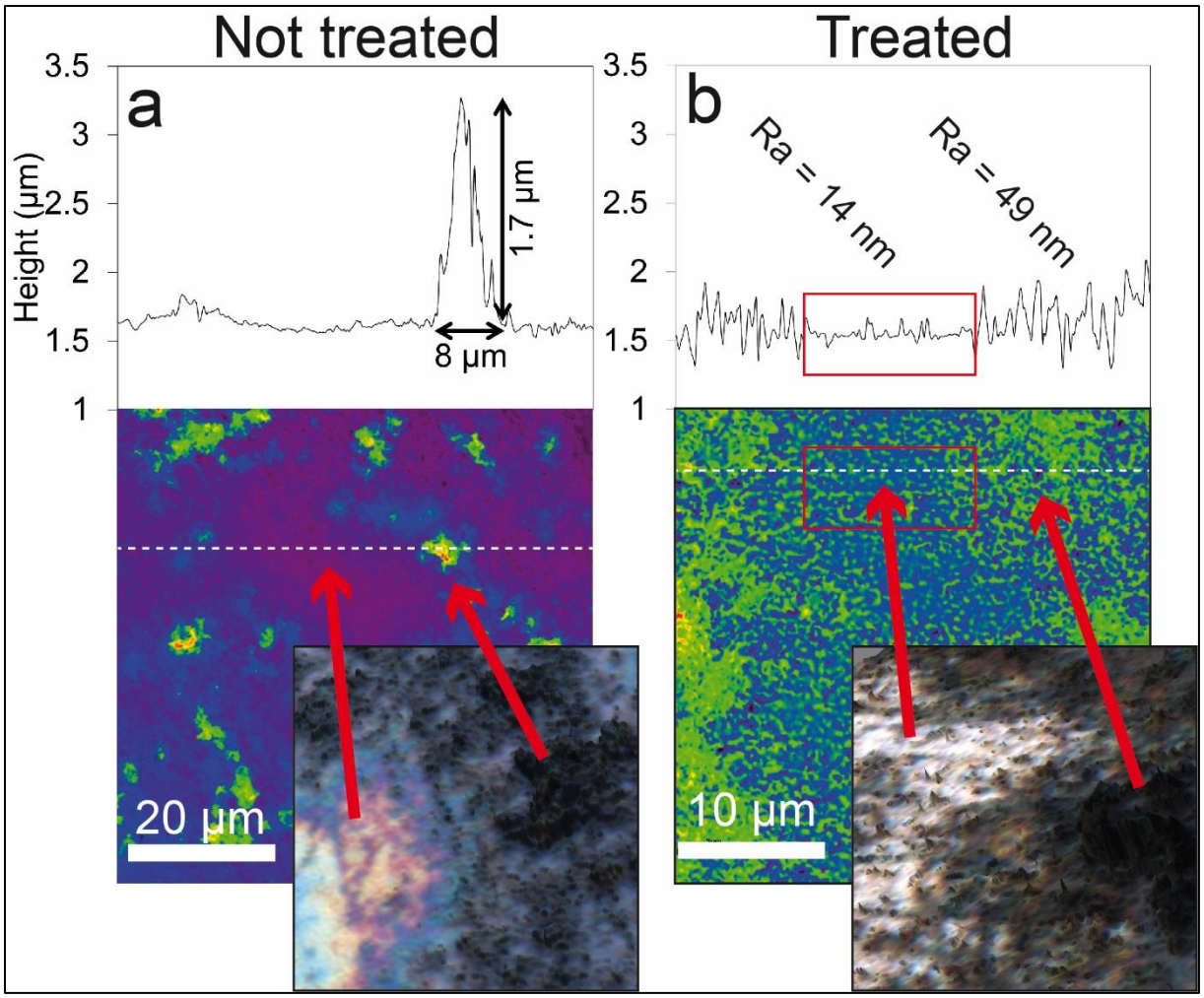

Fig. 5: Topography of corroded Ag925 before and after plasma treatment. a) Height map of the tarnish layer, height profile along a line and 3D visualization of the surface correlating colour with topography; c) Height map, height profile along a line and 3D visualization of the plasma treated surface.

The EDS spectra in Fig. 6a demonstrate that as a consequence of plasma treatment the S-Kα line decreases to some extent while the Cu-L and Ag-L lines increase, suggesting a partial decomposition of the sulphide compounds. During the tarnish of Ag925, bumps rich in Cu and S are being formed [19]. The zones between these bumps are rich in Ag and S. The spectra in Fig. 6b are collected from these 2 zones after plasma treatment. The spectra are collected from a surface tilted at 75° (see Fig. 4g). The Cu-rich bumps still contain substantial amounts of S while the zones between the bumps are poor in S. The chronopotentiometric analyses shown in Figs. 6c and 6d shows several plateaux. Plateau 2 can be attributed to Ag_2S or the overlapping CuS and Cu_2S to plateau 1. Using the transition times given in Fig. 6d, it is clear that Ag_2S/CuS and Cu_2S are reduced by the plasma treatment with a cleaning efficiency of 78% and 35% respectively. Silver sulphide compounds are reduced more efficiently than the copper corrosion products. At the same time, copper oxides are formed during or after the plasma treatment.

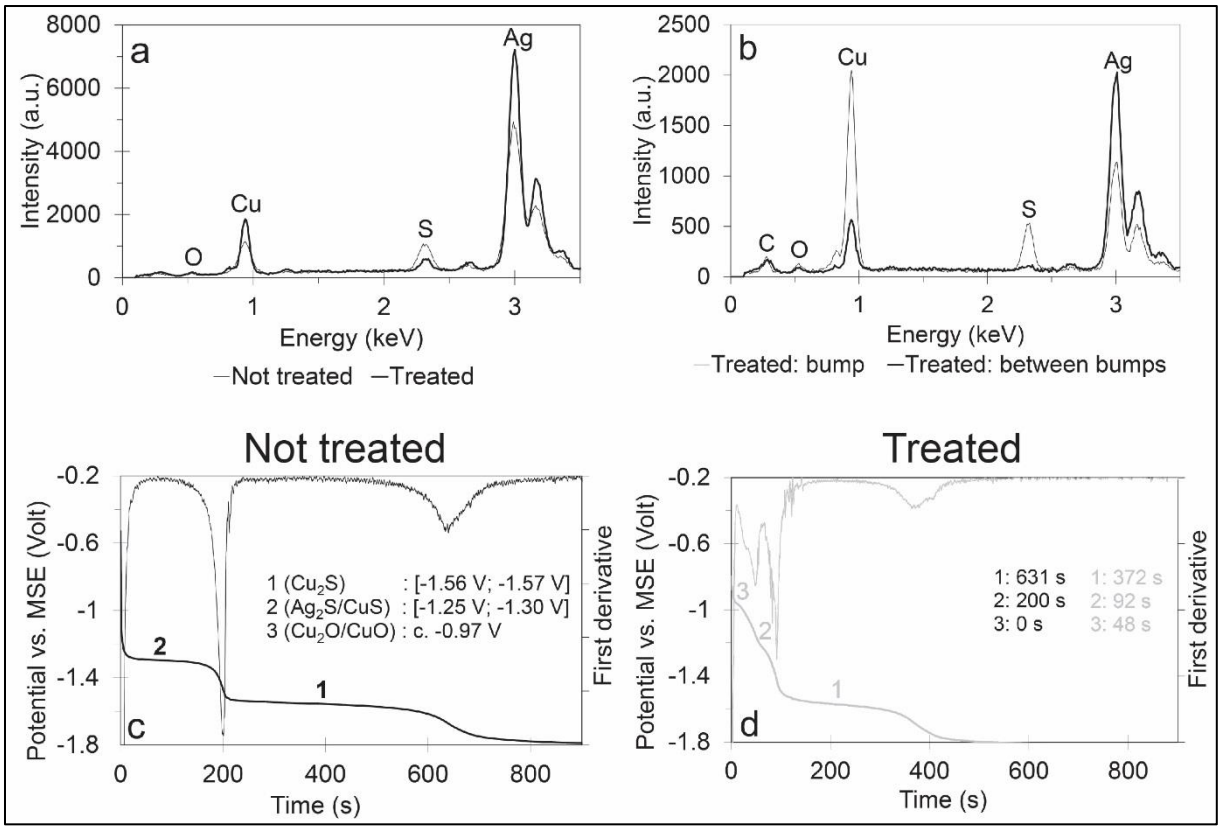

Fig. 6: Surface analyses of Ag925: a) EDS spectra collected from corroded Ag925 before and after plasma treatment; b) EDS spectra collected from the plasma treated surface tilted at 75° from the bump shown in Fig. 4g and of the zone between bumps; c) Chronopotentiometry and corresponding first derivative of corroded Ag925 before plasma treatment; d) Chronopotentiometry and corresponding first derivative of corroded Ag925 after plasma treatment and the transition times of the not treated and treated surface.

4.3. Interaction between the plasma afterglow and Cu999

From a visual inspection of the cleaned Cu999 coupon shown in Fig. 7a, it can be concluded that the plasma treatment is not able to induce any visual change, suggesting that the cleaning efficiency of Cu999 is even worse than that of Ag925.

When the microstructure of the surfaces is evaluated at a microscopic level, considerable changes can be noticed. In the bright field image in Figs. 7b and 7c, the corroded coupon contains black coloured platelets and pink or greenish zones that appear to follow the grain boundaries. The amount of dark platelets seems to be low along the grain boundaries. The plasma treated area (Fig. 7c) does not show these coloured grain boundaries any longer but is pink or greenish over the complete surface. The surface concentration of black platelets seems to be lowered. The secondary electron images of Figs. 7d and 7e show that the lamellar morphology has been transformed in a rougher morphology during plasma treatment.

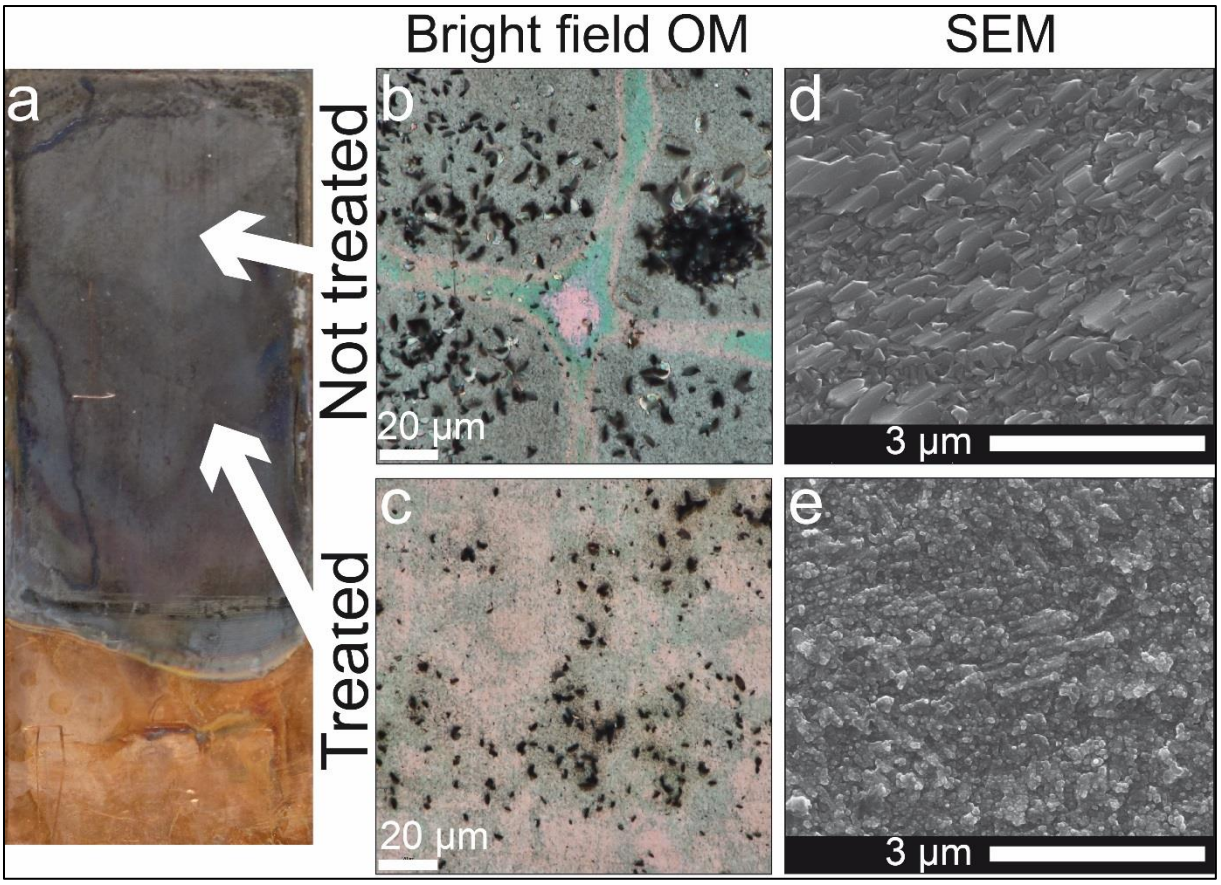

Fig. 7: Inspection of the corroded and plasma treated Cu999 surface. a) The visual appearance of the tarnish layer after plasma treatment is not changed; b) Bright field image of the corroded surface where black platelets and grain boundaries can be seen; c) Bright field image of the corroded surface after plasma treatment where the presence of black platelets is reduced and the complete surface is pinkish/greenish; d) Secondary electron image of the corroded surface visualizing the platelet morphology of the corroded layer; e) Plasma treated tarnish layer showing a rougher surface.

Figs. 8a and 8b shows a Cu999 coupon corroded for a much longer exposure time (i.e., 300 minutes) and treated with a H_2/He afterglow. Fig. 8a visualizes a zone at the border of the plasma treated region, while Fig. 8b is an area in the centre of the plasma treated zone. In both cases, the original corrosion products are covered with a new phase consisting of spheroidal particles. In Fig. 8a, these spheroidal particles are located at the base of the corrosion products while in Fig. 8b they cover the complete surface. A chemical characterization of these spheroidal particles of about 0.1 µm is not possible by means of SEM-EDX due to a lack of depth resolution.

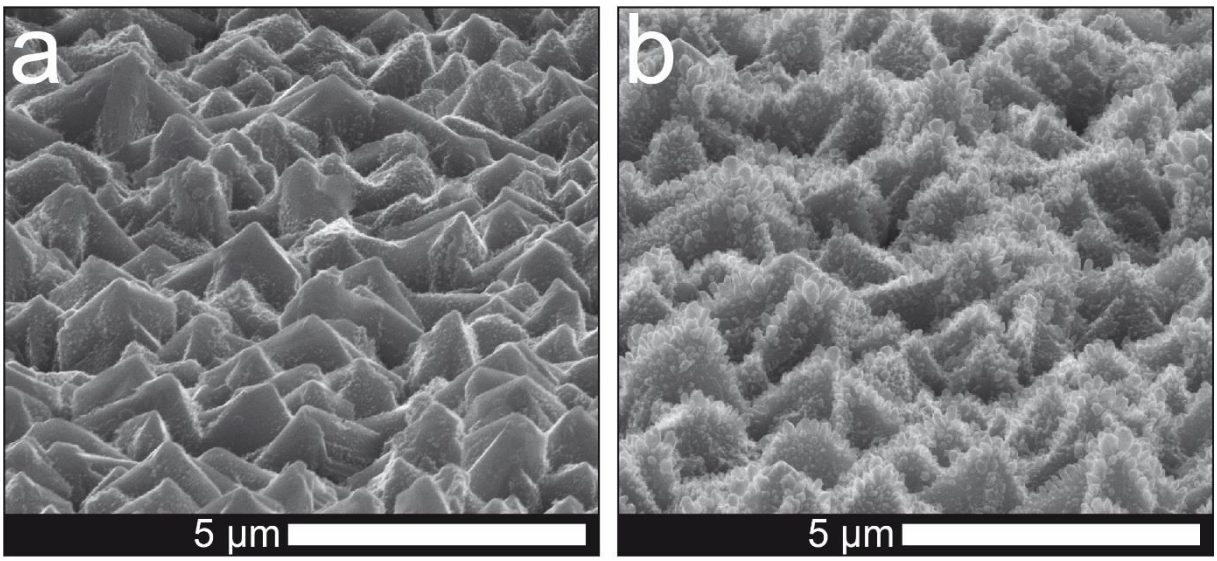

Fig. 8: Three-dimensional view of Cu999 corroded for 300 minutes (instead of 30 minutes) with SEM where secondary electron images are collected from the sample tilted at 75°: a) image collected from the border of the plasma treated zone; b) Image of the same coupon as image a but from the centre of a plasma treated zone showing the presence of a new phase covering the complete surface of the corrosion products.

Fig. 9 shows the first 3 keV of the EDS spectra. The spectra before and after plasma treatment in Fig. 9a suggest that the plasma treatment has a small effect on the tarnish layer. An increase in oxygen content is noticed, although the chronopotentiometric analyses suggest a loss of oxides. Concerning the treated surface, the EDS spectra of Fig. 9b do not show a clear difference between an area containing platelets and an area without platelets. The platelets on top of the tarnish layer are characterized by a S-K:Cu-Kα ratio of about 0.5, while the tarnish layer below has a S-K:Cu-Kα of about 0.35 but this difference is probably due to the contribution of the copper in the underlying metal. The chronopotentiometric analyses shown in Fig. 9c and 9d demonstrate that Cu_2S is partially reduced (cleaning efficiency of 42%), but that during the plasma treatment CuS has been formed (increase of 18%).

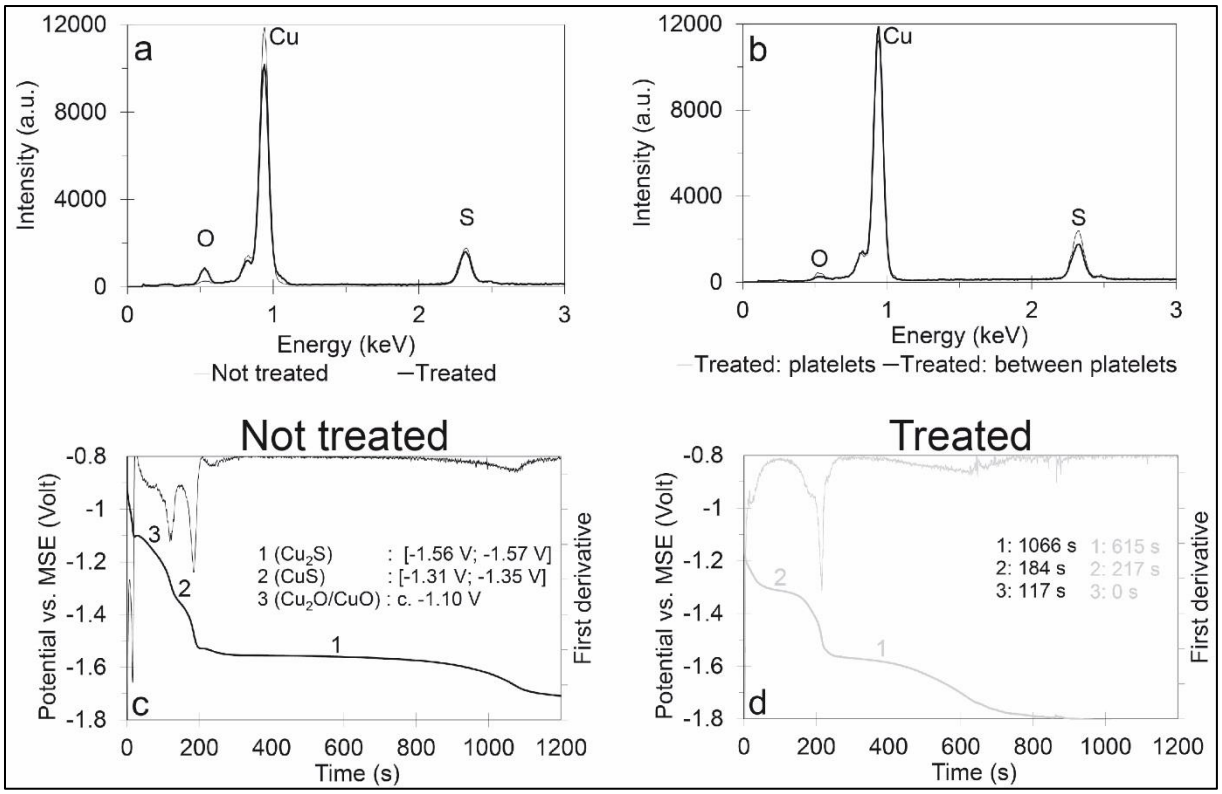

Fig. 9: Surface analyses of Cu999: a) EDS spectra from the corroded surface before and after plasma treatment; b) EDS spectra of a plasma treated area containing platelets and a zone between these platelets; c) Chronopotentiometry of the not treated surface and its first derivative; d) Chronopotentiometry and its first derivative of the plasma treated surface and the transition times from the not treated and treated surface.

5. Discussion

The H_2/He afterglow is able to reduce a substantial amount of the Ag_2S on corroded Ag999. The reducing plasma action seems to be confined in few hundreds nanometre range, maybe helped by the open pores formed during the reduction process. The tarnish layer is transformed through its complete thickness when it is thinner than few hundreds nanometre. For the microscale sulphide grains on the top of the surface, only the surface is affected by the plasma reduction. The oxidized silver is transformed into a porous metallic film. For electrochemical cleaning of corroded silver, a matt grey metallic film is formed as well [4]. When this metallic film remains on the surface, it can be considered as a sacrificial material that will corrode first instead of the underlying bulk metal. Due to its enhanced surface roughness and the accompanying surface area, it is possible that this film corrodes faster than a polished surface. This effect is suggested by the oxygen surface uptake during or after the plasma treatment. In addition, the remaining grains dominate the surface roughness of both corroded and cleaned surfaces so that the original gloss of the sample is not regained. Moreover, the corrosion process seems to etch the metal surface, meaning that the original gloss can only be regained by polishing. The transformation of the tarnish layers on Ag999, Ag925 and Cu999 due to plasma treatment are summarized in Fig. 10.

For Ag925, the tarnish layer consists of Cu-rich bumps with Cu-rich platelets on top and Ag-rich corrosion products in the zones between these bumps. During the cleaning action, the Cu-rich platelets are removed to a large extent while the bumps remain intact. This difference can be due to the different chemical composition but also for the different surface to volume ratio of the structures. The Cu-rich corrosion products are only partially reduced. The Ag-rich corrosion compounds in the valleys are reduced to a large extent and these zones became glossier. The reduction process of metal sulphides is in fact an equilibrium process and silver is more easily reduced than copper [32]. It is at the same time clear that because it is an equilibrium process the removal of H_2S reaction product unbalance the reaction and therefore, the reduction at the surface continues [33]. It is clear that the copper corrosion products on the surface inhibit proper cleaning. It is possible that reduced copper compounds form at the surface a barrier between afterglow and remaining corrosion products. It has to be noted that for more heavily corroded Ag925 sometimes visually better results are obtained because a thin layer of metallic silver covers unreduced corrosion substances. This is especially the case for more extensive corrosion processes because copper corrodes preferentially while Ag-rich corrosion products are only formed in a later stage [19]. It should be remarked that the partial reduction of Cu can result in the formation of a coloured metallic film. Even when this technique would be able to reduce all corrosion products, the result would be unsatisfactory as a result of the yellow surface appearance which is the result of the preferential corrosion of the limited amounts of Cu in silver alloys. In addition, oxides are formed during or after the plasma treatment.

For tarnish layers on top of Cu999, the afterglow is not able to induce any obvious visual effect. However, at the microscopic level changes can be seen. A new phase that has been formed changes the morphology of the surface. Unfortunately, with the analytical techniques used in this investigation that phase cannot be identified, although XPS measurements performed on our samples (not shown here) suggest the presence of metallic copper on top of the surface. These analyses will be the subject of a next article. The dominant compound in the tarnish layer (i.e., Cu_2S) is partially reduced during the plasma treatment but at the same time the amount of CuS is increased. This might be explained by a reaction similar to the thermal decomposition of Cu_2S in the absence of air: $Cu_2S \rightarrow CuS + Cu$ [34]. The analyses performed are unclear if oxides have been removed during plasma treatment as suggested by chronopotentiometry or formed after as suggested by the EDS spectra.

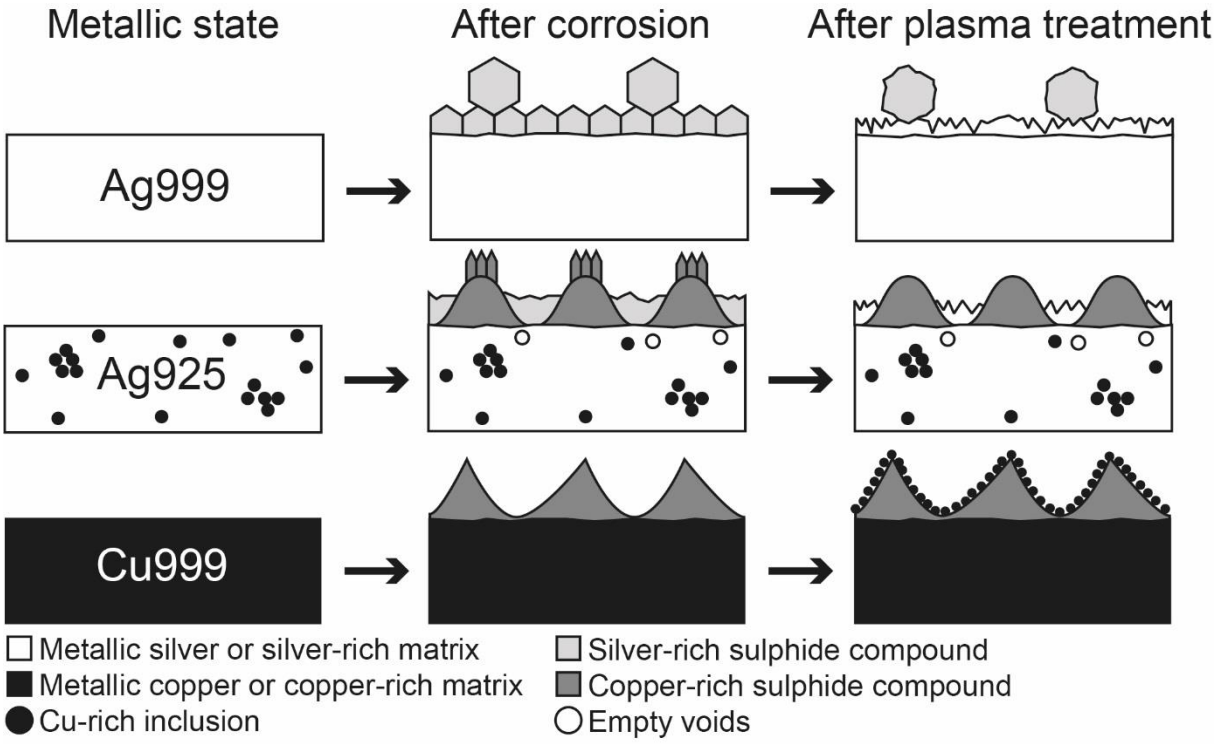

Fig. 10: Schematic representation of Ag999, Ag925 and Cu999 in cross-section in their metallic state characterized by a smooth surface, the surface state after corrosion in a Na_2S solution and the tarnish layer after plasma treatment.

6. Conclusions

The visual appearance of pure silver and silver alloys are expected to be colourless and very glossy. The reductive plasma afterglows are very effective for tarnish layers on Ag999 with a thickness smaller than 220 nm; for tarnish layers that are thicker the cleaning efficiency drops. Unfortunately, even for Ag999 where the sulphide is almost completely removed by a plasma treatment, the original gloss cannot be regained. This is mainly caused by the surface roughness of the metal film or by the surface roughness of the original metal surface due to the etching effect of the corrosion process. Therefore, plasma treatments work best on surfaces of pure silver that are slightly tarnished.

For Ag925, the plasma treatments resulted in a discoloration of the surface. This means that removing all the sulphides on itself is not sufficient to restore the visual appearance of the surface. Plasma treatments are able to transform Ag-rich corrosion products to a large extent and Cu-rich corrosion products to some extent to their metallic state but the original microstructure and topography of the surface is permanently lost during the corrosion process and this cannot be restored with this cleaning technique.

The plasma treatments have no obvious visual impact on corroded Cu999. This demonstrates that the same afterglow has a substantially different effect on sulphide layers on Ag999 and on Cu999. Since most historical ‘silver’ is alloyed with small copper amounts and because this Cu is preferential oxidized during the corrosion process, the removal of tarnish layers on silver alloys with a reducing plasma afterglow at atmospheric pressure remains difficult and unsatisfactory.

Acknowledgements
This work was supported by the EU-FP7 grant PANNA no. 282998 and the STIMPRO project FFB150215 of the University of Antwerp. The authors thank Jean-Christophe Lambrechts for his support in the analyses with the LEXT OLS4100.

References

1. Wharton G, Maish SL, Ginell WS. A comparative study of silver cleaning abrasives. JAIC 1990;29(1):13-32

2. Stambolov T, Removal of Corrosion on an eighteenth-century silver bowl, Stud Conserv, 1966;11(1):37-44

3. MacLeod ID, North NA., Conservation of corroded silver, Stud Conserv 1979;24(4):165-170

4. Novakovic J, Vassiliou P, Georgiza E. Electrochemical Cleaning of Artificially Tarnished Silver. Int J Electrochem Sci 2013;8:7223-7232

5. Degrigny C, Jeanneret R, Witschard D, Baudin C, Bussy G, Carrel H, A new electrolytic pencil for the local cleaning of silver tarnish, Stud Conserv 2016;61(3):162-173

6. Barger MS, Krishnaswamy SV, Messier R. The cleaning of daguerreotypes: comparison of cleaning methods'. JAIC 1982;22:13-24

7. Turovets I, Maggen M, Lewis A, Cleaning of daguerreotypes with an excimer laser. Stud Conserv 1998;43:89-100

8. Daniels V, Holland L, Pascoe MW. Gas plasma reactions for the conservation of antiquities, Stud Conserv 1979;24(2):85-92

9. Goossens O, Dekempeneer E, Vangeneugden D, Van de Leest R, Leys C. Application of atmospheric pressure dielectric barrier discharges in deposition, cleaning and activation. Surf Coat Technol 2001;142-144:474-481

10. Saettone EAO, da Matta JAS, Alva W, Chubaci JFO, Fantini MCA, Galvao RMO, Kiyohara P, Tabacniks MH. Plasma cleaning and analysis of archeological artefacts from Sipan, J Physics D: Appl Phys 2003;36:842-848

11. Schmidt-Ott K. Plasma-Reduction: Its Potential for Use in the Conservation of Metals, Proceedings of Metal 2004, National Museum of Australia Canberra ACT, Canberra, 4-8 October 2004, 235-246

12. Goras BT, Ioanid EG, Rusu D, Goras L. Optical evaluation of heritage silver coin plasma cleaning using statistical methods. Optoelectronics Adv Mater – Rap Comm 2010;4(12):2157-2161

13. Ioanid EG, Ioanid A, Rusu DE, Doroftei F. Surface investigation of some medieval silver coins cleaned in high-frequency cold plasma. J Cult Herit 2011;12: 220–226

14. Grassini S, Angelini E, Mao Y, Novakovic J, Vassiliou P. Aesthetic coatings for silver based alloys with improved protection efficiency. Prog Org Coat 2011;72:131-137

15. Daniels V. Plasma reduction of silver tarnish on daguerreotypes. Stud Conserv 1981;26:45-49

16. Ioanid EG, Ioanid A, Rusu DE, Popescu CM, Stoica I. Surface changes upon high-frequency plasma treatment of heritage photographs. J Cult Herit 2011;12:399–407

17. Boselli M, Chiavari C, Colombo V, Gherardi M, Martini C, Rotundo F. Atmospheric pressure non-equilibrium plasma cleaning of 19th century daguerreotypes. Plasma Proc Polym 2016;14(3), DOI: 10.1002/ppap.201600027

18. Grieten E, Schalm O, Tack P, Bauters S, Storme P, Gauquelin N, Caen J, Patelli A, Vincze L. Reclaiming the image of daguerreotypes: Characterization of the corroded surface before and after atmospheric plasma treatment, J Cult Herit, in press

19. Schalm O, Crabbé A, Storme P, Wiesinger R, Gambirasi A, Grieten E, Tack P, Bauters S, Kleber Ch, Favaro M, Schryvers D, Vincze L, Terryn H, Patelli A. The corrosion process of sterling silver exposed to a Na_2S solution: monitoring and characterizing the complex surface evolution using a multi-analytical approach, Appl Phys A 2016;122(903),DOI:10.1007/s00339-016-0436-6

20. Storme P, Schalm O, Wiesinger R. The sulfidation process of sterling silver in different corrosive environments: impact of the process on the surface films formed and consequences for the conservation-restoration community, Herit Sci 2015;3(25), DOI:10.1186/s40494-015-0054-1

21. Faltermeier RB. A corrosion inhibitor test for copper-based artifacts. Stud Conserv. 1998;44(2):121-128

22. Evesque M, Keddam M, Takenouti H. The formation of self-assembling membrane of hexadecane-thiol on silver to prevent the tarnishing. Electrochim Acta 2004;49(17-18):2937-2943

23. Ravines P, Wiegandt R, Hailstone R, Romer G, Optical and surface metrology applied to daguerreotypes, In Townsend JH, Toniolo L, Cappitelli F (eds) Conservation Science 2007:Papers from the Conference held in Milan, Italy 24–26 May 2007, Archetype Publications, London, pp. 131-139

24. Ravines P, Chen JJ, Wichern CM. Surface characterization and monitoring of surface changes after conservation treatments of silver gelatin photographic papers using confocal microscopy. Scanning 2010;32:122-123

25. Norm NBN EN ISO 8891:2000, Dental casting alloys with noble metal content of at least 25% but less than 75%, Annex B Tarnish testing - sodium sulfide test, p. 8

26. Van Laer W, Weg-Wyzer voor aankoomende Gouden Zilversmeeden (in Dutch), Amsterdam (1725), reprinted by De Tijdstroom, Lochem (1967).

27. Hammes J, Goud Zilver Edelstenen (in Dutch), Amsterdam: De Technische Boekhandel H. Stam, 1943

28. Slesinski, W, Entwicklung der Reinigungsmethoden von Silberzeugnissen, in Jaro M, Eri I. (ed.) Conservation of Metals: Problems in the treatment of metal-organic and metal-inorganic composite objects. International restorer seminar. Veszprém, Hungary, 1-10 July 1989, pp. 108-109

29. ASTM B825-02. Standard Test Method for Coulometric Reduction of Surface Films on Metallic Test Samples. =

30. Degrigny C., Wéry M., Vescoli V., Blengino, M. 1996. Altération et nettoyage de pièces en argent doré, Stud Conserv 1996;41:170–178

31. Wei W., Gerritsen I., Von Waldthausen C., Re-examining the (electro-)chemical cleaning of daguerreotypes: microscopic change vs. macroscopic perception, Topics in Photographic Preservation, 2011;14, 24-40

32. Zuckerman JJ, Hagen AP (eds). Inorganic Reactions and Methods, Volume 1: The formation of bonds with hydrogen (Part 1), VCH Publishers, 1986

33. Habashi F, Dugdale R. The reduction of sulphide minerals by hydrogen in presence of lime, Metall Trans 1973;4:1865-1871

34. Patnaik, P., Handbook of inorganic chemicals, McGraw-Hill, New York, 2003, p. 277